Bioorganic Chemistry 83 (2019) 87–97

Contents lists available at ScienceDirect

Bioorganic Chemistry

journal homepage: www.elsevier.com/locate/bioorg

Design, synthesis, structural characterization and *in vitro* evaluation of new 1,4-disubstituted-1,2,3-triazole derivatives against glioblastoma cells

Veronica D. da Silva[a], Bruna M. de Faria[b], Eduardo Colombo[a], Lucas Ascari[c], Gabriella P.A. Freitas[b], Leonã S. Flores[d], Yraima Cordeiro[c], Luciana Romão[b], Camilla D. Buarque[a,*]

[a] *Laboratório de Síntese orgânica, Pontifícia Universidade Católica do Rio de Janeiro, 22451-900 Rio de Janeiro, RJ, Brazil*
[b] *Instituto de Ciências Biomédicas, Universidade Federal do Rio de Janeiro, 21941-902 Rio de Janeiro, RJ, Brazil*
[c] *Faculdade de Farmácia, UFRJ, RJ 21941-902, Brazil*
[d] *Laboratório de Difração de raios X, UFJF, MG 36036-900, Brazil*

ARTICLE INFO

InChIKeys:
ZBMSMTCPPZJWEP-DBMXBCQFSA-N
MQHUQYSZXRGRAR-UHFFFAOYSA-N
HLLRMTAVRDWGTD-UHFFFAOYSA-N
ZQWURLIKNXEZDT-UHFFFAOYSA-N
PLMRVHURTZLGRK-UHFFFAOYSA-N
BPUKUAOGINJQIA-UHFFFAOYSA-N
PFHZPNNQAIDXLS-UHFFFAOYSA-N
VQXPESGWEBJOLM-UHFFFAOYSA-N
FNLJQDNWPOTMEK-UHFFFAOYSA-N
IFFKXWJZVGMRAW-HZHRSRAPSA-N
ISOSTYYBZMWTOV-BUVRLJJBSA-N
WRMXGIHUGZDXRY-UHFFFAOYSA-N
OOZMSGLPMDLHKT-WAJJMWJGSA-N
Keywords:
Azide-alkyne cycloaddition
1,4-disubstituted-1,2,3-triazoles
Tosyl-hydrazone
Glioblastoma
Drug-resistant
Drug score
Cancer
Crystal structure

ABSTRACT

A new series of 1,4-disubstituted-1,2,3-triazole derivatives were synthesized through the copper-catalyzed azide-alkyne 1,3-dipolar cycloaddition (Click chemistry) and their inhibitory activities were evaluated against different human glioblastoma (GBM) cell lines, including highly drug-resistant human cell lines GBM02, GBM95. The most effective compounds were **9d,** containing the methylenoxy moiety linked to triazole and the tosyl-hydrazone group, and the symmetrical bis-triazole **10a**, also containing methylenoxy moiety linked to triazole. Single crystal X-ray diffraction analysis was employed for structural elucidation of compound **9d**. *In silico* analyses of physicochemical, pharmacokinetic, and toxicological properties suggest that compounds **8a, 8b, 8c, 9d**, and **10a** are potential candidates for central nervous system-acting drugs.

1. Introduction

Glioblastoma (GBM) is one of the most aggressive human cancers in the brain [1]. Although new therapeutics are currently being tested in clinical trials, GBMs are still highly drug-resistant, limiting the effectiveness of chemotherapy [1]. Examples of new 4-anilinoquinazolines are erlotinib, gefitinib, acting as inhibitors of epidermal growth factor receptor (EGFR) [2], and cediranib, pazopanib and sorafenib acting as tyrosine kinase inhibitors. Nevertheless, temozolomide (TMZ) (**1**) (Fig. 1) is the first choice chemotherapeutic agent for the treatment of GBM. Due to its small size and lipophilic features, the drug is able to cross the blood-brain barrier and acts as a DNA alkylating agent [3]. However, the therapeutic efficacy of TMZ is unsatisfactory against the invasive and resistant nature of GBM [4], showing high IC_{50} values of 330 μM against U87 cells, requiring high concentrations of the drug to current treatment of GBM [5]. The well-known scaffold 1,2,3-triazol, present in several heterocyclic compounds, harbors a broad spectrum of biological applications [6], such as anti-tubercular [7], antibacterial and antifungal [8,9], anticonvulsant [10], antiviral [11,12], anticancer [13,14] activities, among others. 1,2,3-triazoles are classified within

* Corresponding author.
E-mail address: camilla-buarque@puc-rio.br (C.D. Buarque).

https://doi.org/10.1016/j.bioorg.2018.10.003
Received 7 June 2018; Received in revised form 25 September 2018; Accepted 4 October 2018
Available online 11 October 2018
0045-2068/

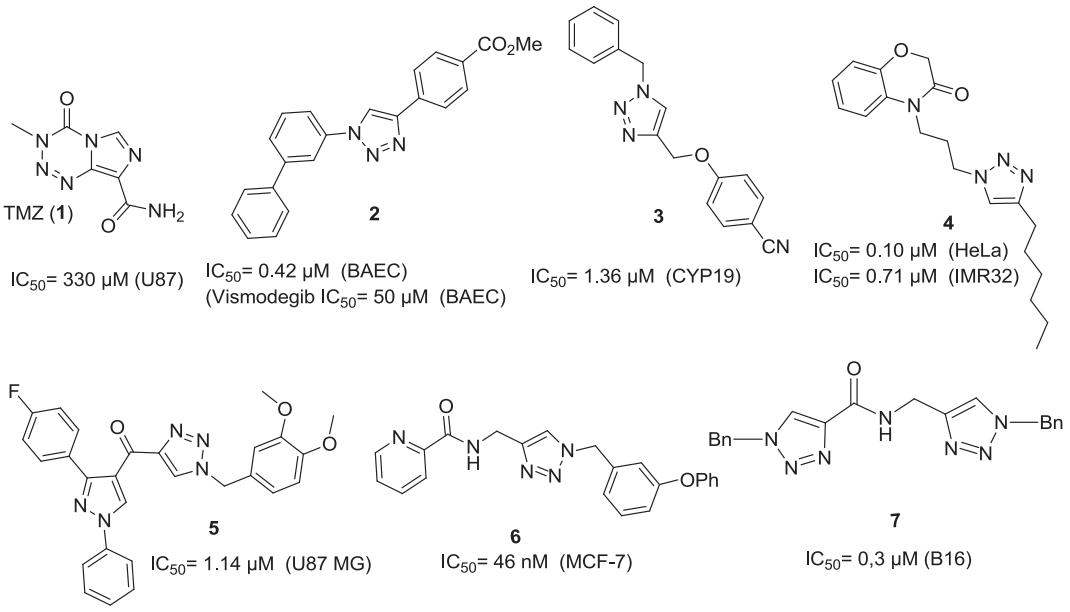

Fig. 1. Commercial drug TMZ (**1**) and selected examples of 1,4-disubstituted-1,2,3-triazoles (**2–7**) with anticancer activity.

the most common amide bond isosters since they present a good overlap with the amide-binding moiety [15]. In particular, 1,2,3-triazoles can actively participate in dipole-dipole interactions due to its strong dipole moment, are stable for oxidative and reducing conditions and the 1,2,3-triazole ring is not protonated in physiological pH due to its low basicity as well as may mimic the features of different functional groups [16].

There are some examples of 1,4-disubstituted-1,2,3-triazoles with anticancer activity. For example, the triazole-based vismodegib analog (**2**) had the potency increased against different cancer and endothelial cell lines when compared to vismodegib, a synthetic Hedgehog signaling pathway inhibitor. This compound was over 50 times more active against bovine aortic endothelial cells (BAEC) than original vismodegib, due to the isosteric exchange of the amide moiety [17]. A series of 1,4-disubstituted-1,2,3-triazoles was tested as aromatase inhibitors for the treatment of breast cancer and compound **3** showed the best result, with IC_{50} = 1.36 μM [18]. Using the same chemical approach, 1,2,3-triazole-1,4-benzoxazine hybrids were synthesized and evaluated for anticancer activity against HeLa (cervical), MIAPACA (pancreatic), MDA-MB-231 (breast) and IMR32 (neuroblastome) cell lines. Compound **4** presented the best result with IC_{50} values ranging from 0.1 to 1.1 μM, against the above cited cell lines [13]. A series of pyrazolo-triazole hybrids were synthesized and evaluated for anticancer activity against four tumor cell lines, HT-29 (colon), PC-3 (prostate), A549 (lung), and U87MG (glioblastoma) cells. Compound **5** presented the best result against U87MG cell lines [19]. Other compounds based on 1,2,3-triazoles such as **6** presented anticancer activity against breast cancer (MCF-7) [20]. Some bis-heterocycles with wide range of applications also have gained importance in medicinal chemistry in the literature. For example, some sulfone/sulfonamide-linked bis(oxadiazoles), bis(thiadiazoles) and bis(triazoles) presented antioxidant activity [21]. The 1,2,3-bis-1,2,3-triazole (**7**) presented anticancer activity against B16 melanoma, where the bis-triazole moiety was more active than mono-triazole used for its preparation [22]. Moreover, there are some bis-triazole-based commercial drugs available in the market, for example Fluconazole, Itraconazole and Posaconazole were used as antifungal drugs and vorozole as antineoplastic drug. [23] Fig. 1 describes some examples of these potentially bioactive triazoles.

Triazoles with different pattern of substitution were also described to present cytotoxic effects against GBM cell lines [19,24,25]. Ribavirin, for example, is a 1,3-disubstituted-1,2,4-triazole used for the treatment of seven different GBM cell lines presented IC_{50} values ranging from ~30 to 660 μM [25].

The potential of 1,4-disubstituted-1,2,3-triazoles as antineoplastic substances prompted us to design and synthetize new compounds as prototypes for GBM therapy, including drug-resistance cell lines. In this manuscript, we report the synthesis of 1,4 disubstituted-1,2,3-triazole based compounds **8–10** and the evaluation of their potential anti-GBM activity (Fig. 2).

Compounds **8a-c** and **9a-d** were designed to correlate the effect of exchange of functional groups of aldehydes, an electrophilic group that can form a schiff base with DNA [26,27], by classical pharmacophoric groups, designed to obtain innovative bifunctional drugs since triazoles can work as special ligand by connecting these one. Sulphonylhydrazones and hydrazones, on the other hand, are known to inhibit several enzymes involved in cancer disease [2,7,28–30], and the polar group CHF_2 can act as an unusual hydrogen bond donor being a bioisostere of OH group [31].

The effect of substitutions at the A and C-rings on the cytotoxicity against human GBM cell lines (GBM02, GBM95) and the commercial cell U87, was also evaluated for compounds **8a-e**. In order to understand the role of spacer methylenoxy moiety in compounds **8a-e**, derivative **8f** was synthesized. Since 1,2,3-triazoles gained importance for medicinal chemistry, investigation of bis-triazoles **10a**, **10b** and **10c** easily prepared from bis-alkynes derived from resorcinol was undertaken.

Additionally, the compounds were subjected to a computational prediction of their physicochemical, pharmacokinetic, and toxicological properties. Compounds **8a**, **8b**, **8c**, **9d**, and **10a** showed the best results both *in vitro* and *in silico*.

2. Results and discussion

2.1. Synthesis of 1,4-disubstituted-1,2,3-triazoles

The 1,4-disubstituted-1,2,3-triazoles (**8a-d**) were obtained in high yields by the copper-catalyzed azide-alkyne click chemistry reaction between aryl-azides (**13a-c**) and propargyl-phenols (**12a-d**) (Scheme 1). using one equivalent of corresponding azides and alkynes, except for compound (**10a**), whereas two equivalents of the azide (**13a**) was used [32]. These propargyl-phenols were prepared by alkylation of phenols (**11a-d**) with propargyl bromide in the presence of K_2CO_3 as a base in

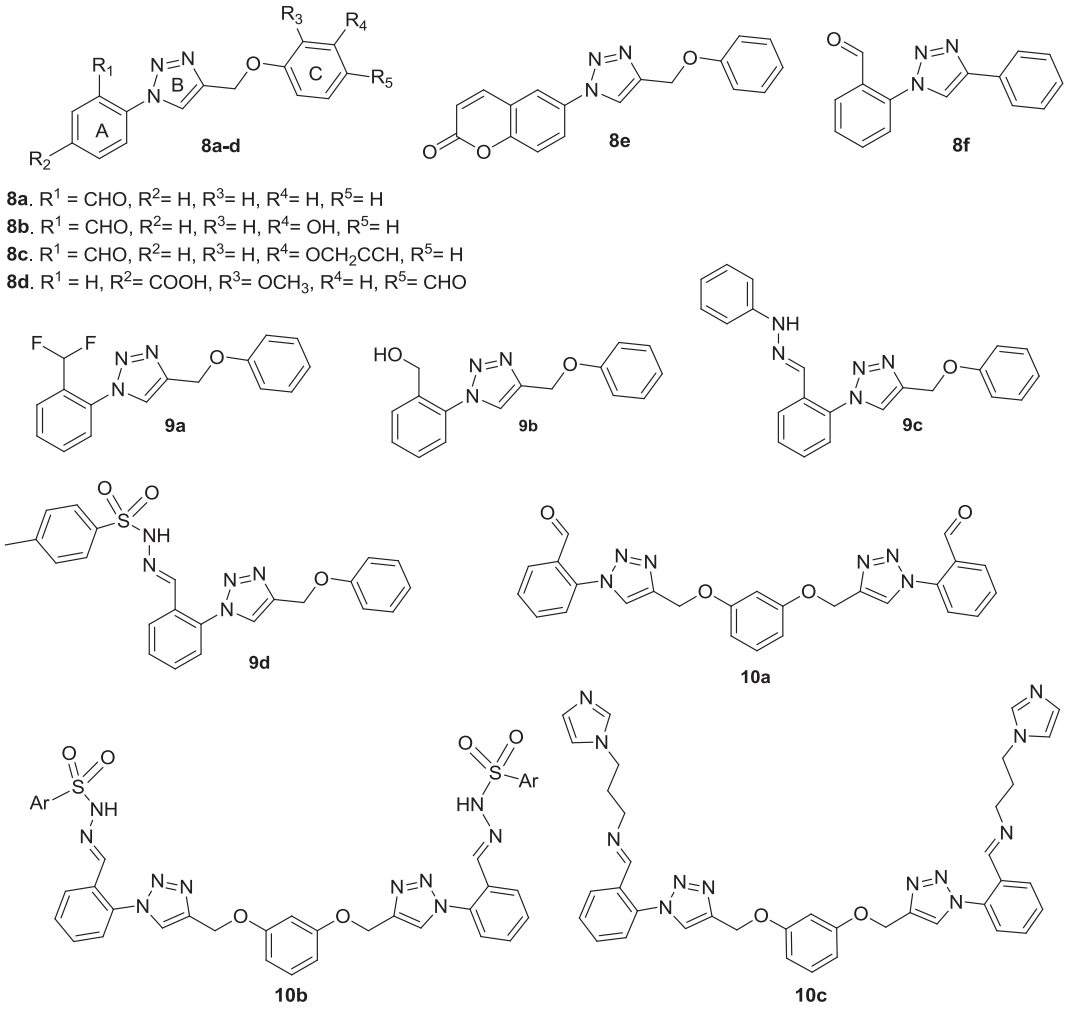

Fig. 2. 1,4-disubstituted-1,2,3- triazoles synthesized in this work.

acetonitrile (CH_3CN) affording the corresponding products in yields ranging from 30% to 80%. 2-azido-benzaldehyde (**13a**) was obtained by reaction of 2-nitro-benzaldeyde with sodium azide in 60% yield [33]. The other aryl-azides (**13b-c**) were prepared from commercial anilines by diazotization reaction with $NaNO_2$ followed by substitution with sodium azide (NaN_3) in 85 and 94% yield, respectively [34]. The chemical structures of the aryl-azides were confirmed by FT-IR and ^1H NMR. The FT-IR analysis showed a strong absorption band near to 2100 cm^{-1}, attributed to the stretching vibrations of the azido group. Triazole **8f,** which lacks the methylenomethoxy moiety, was also prepared by click chemistry reaction between phenylacetylene (**12e**) with aryl-azide **13a** [35]. Compounds (**8a-f**) were characterized by ^1H NMR, ^{13}C NMR and mass spectrometry. The ^1H NMR spectrum exhibited a singlet signal at δ 5.3 ppm, relative to the methylene group (CH_2). In addition, the appearance of the sharp singlet signal in the region δ 8.03–9.10 ppm confirmed the presence of triazole proton. In ^{13}C NMR, carbon signals characteristic of the methylene group and the triazole ring (C4) were observed around δ 61.14–62.87 and 144.05–148.56 ppm, respectively.

Alcohol (**9b**) was prepared by reduction of **8a** with $NaBH_4$ in methanol and the product was obtained in 65% yield (Scheme 2). The fluorinated compound **9a** was obtained in 72% yield by electrophilic fluorination in the presence of diethylaminosulfur trifluoride (DAST). Compound **9c** was obtained by reaction of **8a** with phenyl-hydrazine in 70% yield and compounds **9d** and **10b** were obtained by reaction of **10a** with tosyl- hydrazine to afford the corresponding hydrazones in 65% and 76% yields, respectively. Compound **10c** was obtained by reaction of **10a** with 3-aminopropyl-imidazole in 60% yield.

Single crystal X-ray diffraction analysis was employed for structural elucidation of compound **9d**. The crystal and instrumental parameters used in the unit cell determination, the data collection, and structure refinement parameters are presented in Table S1 while selected bond distances and angles in Table S2 (supplementary material). The *E*-configuration of the tosyl-hydrazone was observed in the solid crystalline state, based on C8/N2/N1 iminic bond and involving a C9-C8-N2-N1 torsion angle of −175.77 (1). The extended conformation of **9d** molecule is assembled on a supramolecular environment involving considerable classical hydrogen bonds N1—H1N···O3^{i}; d(H···A) = 2.05 Å and ∠(D-H···A) = 171°:. *i* = −*x*, −*y*, −*z*. Some weak forces are showed as C20—H20···N4^{i} and C15—H15···O1^{ii} non-classical hydrogen bonds (*ii* = −*x*, *1* − *y*, −*z*). The geometry adopted by approximation of toluene rings suggests a weak π-π stacking interaction [36–38] (Fig. 3). The analysis of full interaction maps for conformation adopted by **9d** (Fig. 4a) indicates large H-bond acceptor peaks directing for the tosyl and azide groups suggesting a stronger acceptor region. Parallel, a smaller donor peak directed to toluene ring may indicate a propensity to unconventional hydrogen bond. Additionally, the π-π stacking interaction only has been observed on toluene ring, which is the unique ring group unsatisfied by hydrophobic region probes (Fig. 4b). Therefore, the principal contact interactions observed are unsatisfied by the region probes and it may suggest a possible metastability of the crystal, in the sense of the polymorphic structure formation.

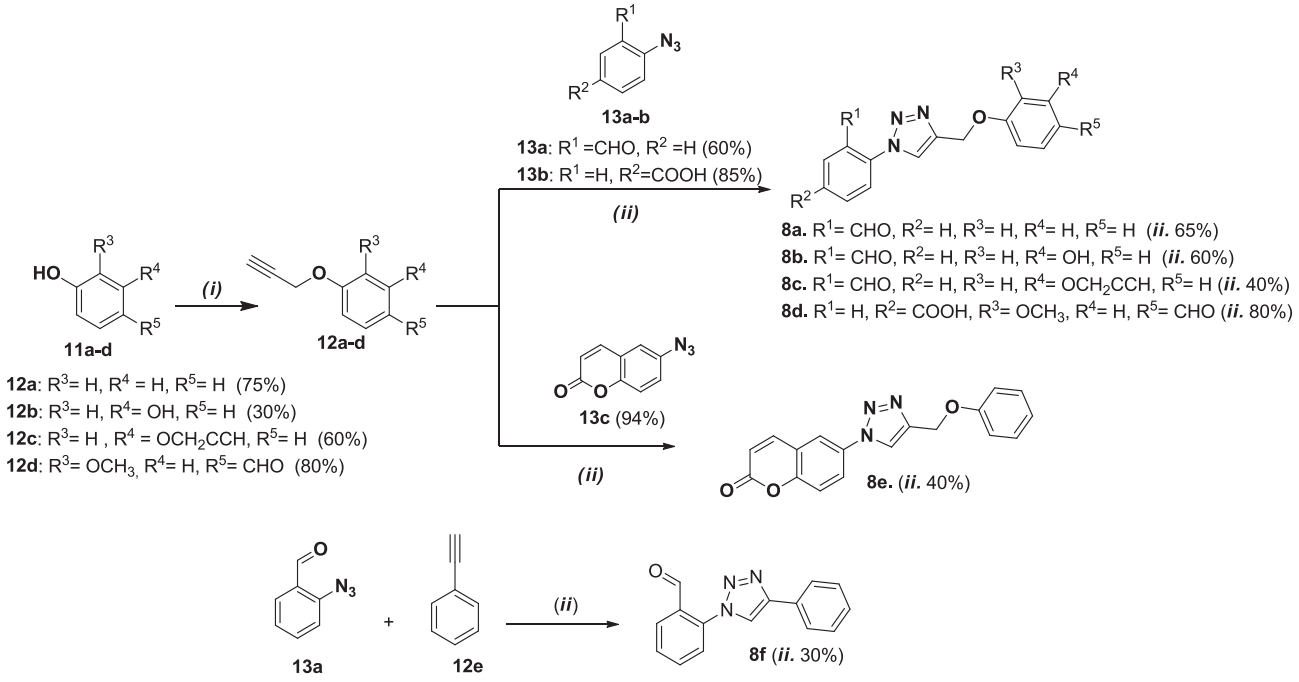

Reagents and conditions: (*i*) propargyl bromide, K_2CO_3, CH_3CN reflux, 4h. (*ii*) $CuSO_4.5H_2O$, 1 mol%, sodium ascorbate 10 mol%, t-BuOH/H_2O 1:1, t.a. 8h.

Scheme 1. Synthesis of the 1,4-disubstituted-1,2,3-triazoles compounds (**8a–f**).

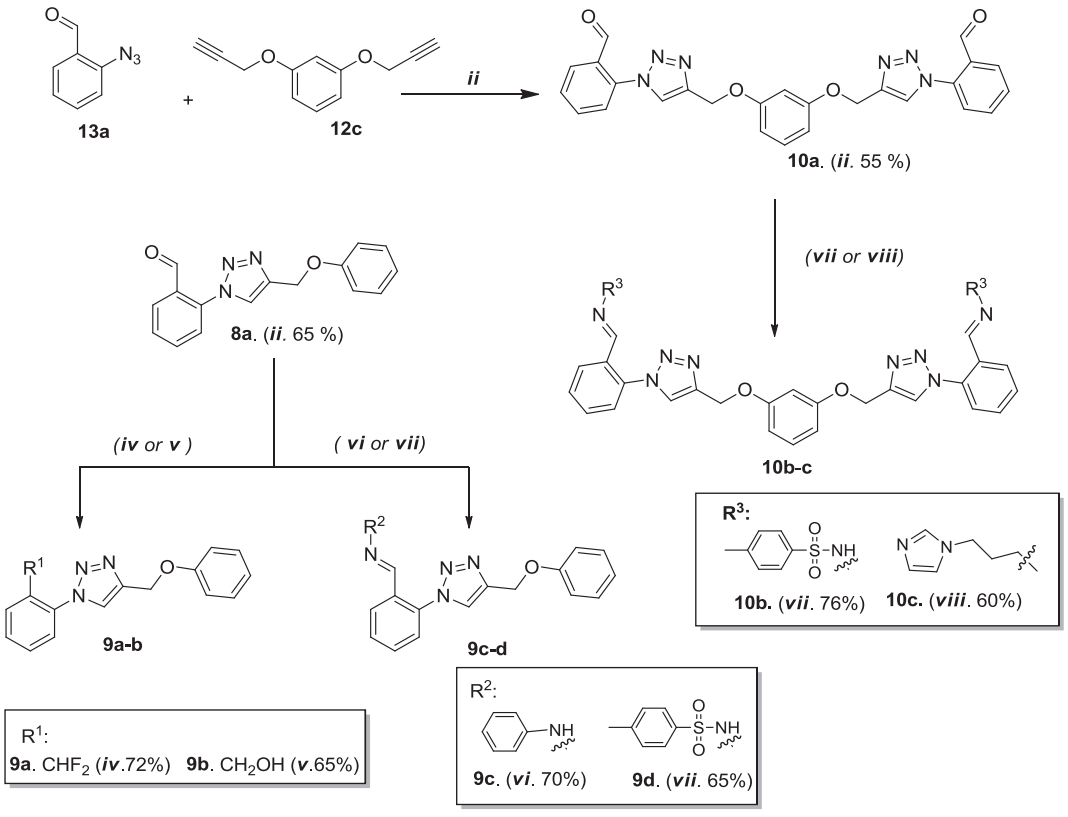

Reagents and conditions:(*ii*) $CuSO_4.5H_2O$, 1 mol%, sodium ascorbate 10 mol%, *t*-BuOH/H_2O 1:1, t.a. (*iv*) DAST,CH_2Cl_2 dry, rt, 24h. (*v*) $NaBH_4$, MeOH, rt , 0.5h.(*vi*) phenyl-hydrazine, MeOH reflux, 2h. (*vii*) tosyl-hydrazine, MeOH reflux, 2h. (*viii*) 1-(3-aminopropyl)imidazole ($C_3H_4N_2C_3H_6$), MeOH reflux, 2h.

Scheme 2. Synthesis of the compound (**10a**) and triazole derivatives (**9a-d** and **10b-c**).

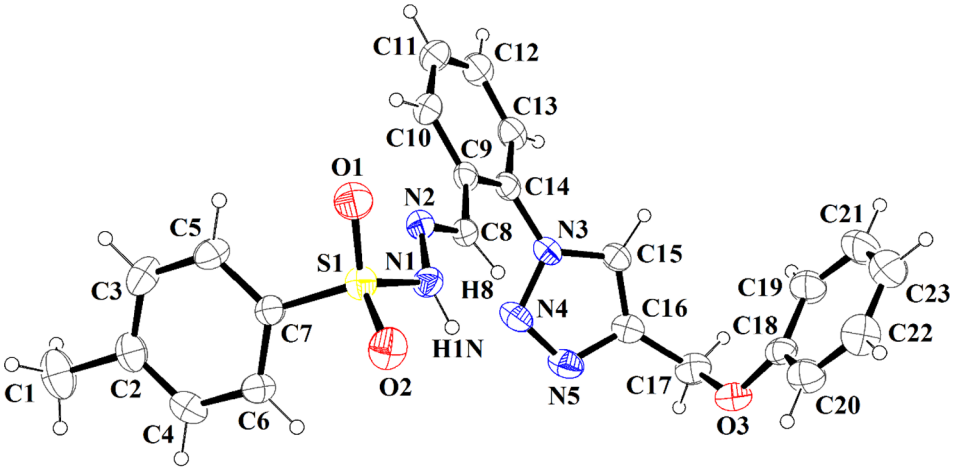

Fig. 3. ORTEP representation of the asymmetric unit of **9d** crystal structure. Ellipsoids are shown at the 30% of probability level.

2.2. Biological evaluation

2.2.1. Cytotoxicity of *8a-f, 9a-d and 10a-c* compounds in GBM cells

In order to evaluate the antitumor potential of triazole compounds against GBM cells, U87, GBM02 and GBM95 cell lines were incubated with 10, 50 or 100 μM of each of the compounds for 48 and 72 h. Treatments **8a, 8b, 8c, 9d, 10a** and **10c** showed the most efficient cytotoxic effects (Fig. 5 and Table 1). These compounds were able to reduce viability of the three GBM cell lines tested, in concentration- and time-dependent manners (Fig. 5). Therefore, the most prominent results were detected in treatments with 100 μM of compounds for 72 h. Thus, **8a**, **8b**, **8c**, **9d**, **10a** and **10c** are cytotoxic to all three GBM cell lines tested, presenting IC_{50} values ranging from ~20 to 190 μM for 72 h treatments (Table 1). In order to compare the antitumor potencial of triazoles with the current chemotherapeutic used in the treatment of GBM patients, we treated GBM cells with 100, 500 and 1000 μM **TMZ** for 48 and 72 h and measured cell viability. We observed that **TMZ** treatment reduced viability of GBM02 and GBM95 presenting an IC_{50} values of 624.8 and 1132 μM in the 72-h treatments. However, the same treatment was not able to reduce the viability of U87 lineage cells (Fig. 7 and Table 1). Our results suggest that the triazole compounds in these studies have a higher cytotoxic potential than the current chemotherapeutic agent (**TMZ**).

We next investigated whether triazole compounds act selectively against GBM cells. For that, we treated human astrocyte cells with the same set of treatments used before. All triazole compounds, except for **10c**, did not induce significant reductions in astrocytes viability (Fig. 6). The **10c** compound was cytotoxic to astrocytes, reducing 58.6% of the cellular viability (Fig. 6). We also observed that the treatment with **TMZ** reduced the viability of human astrocytes, exhibiting an IC_{50} of 993.3 μM 48 h e 948.8 μM 72 h (Fig. 7 and Table 1).

Thus, **8a**, **8b**, **8c**, **9d, and 10a** presented selectivity effect, exhibiting antitumoral activity without being cytotoxic to healthy astrocytes at the concentrations used in our work.

In agreement with our results, it has been shown that treatment with different concentrations of 1,2,4-triazole[3,4-*b*]-1,3,4-thiadiazine derivative reduced T98G GBM cell line viability [24] in concentration and time-dependent manners. Ribavirin treatments in seven different GBM cell lines presented IC_{50} values ranging from ~30 to 660 μM [25]. Moreover, when we compare our results with the *in vitro* effect of **TMZ**, the current chemotherapeutic agent used in patients with GBM, we can see that **8a**, **8b**, **8c**, **9d**, **10a** and **10c** showed more cytotoxic potential and, differently from **TMZ**, the compounds **8a**, **8b**, **8c**, **9d** and **10a** were not cytotoxic for human astrocytes. Therefore, as we observed in our results, other studies also showed low efficiency of **TMZ** *in vitro*. Castro and collaborators demonstrated that the IC_{50} of **TMZ** for U87 cells after 24 h of treatment is 330 μM [5] and for T98G and U138 cells after 72 h of treatment is higher than 500 μM [39]. Previous studies from our group showed that 500 μM of **TMZ** treatment for 48 h reduced only 29.5% ± 6.7% of U87 cells viability [40] and 1000 μM of **TMZ** did not reduce GBM02 and GBM95 cells viability after 24 h of incubation [41,42].

The best biological response against human tumor cell lines (U87, GBM95 and GBM02) is related to the symmetric aldehyde triazole

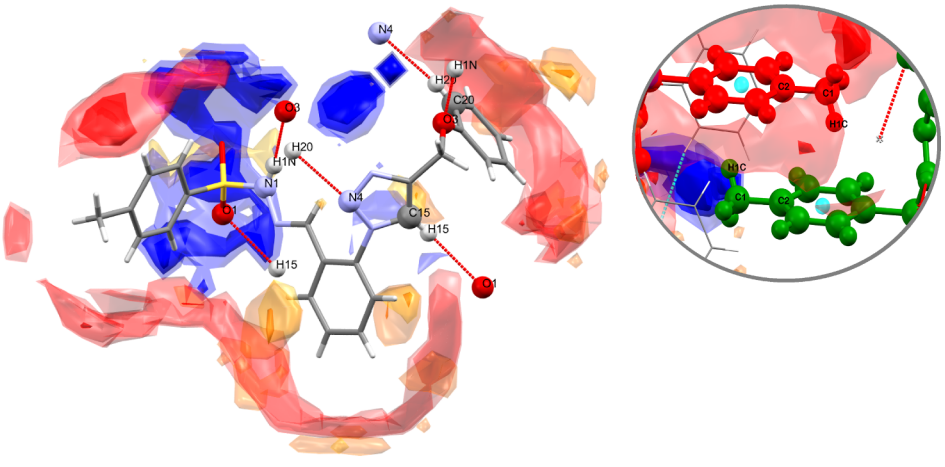

(a) *(b)*

Fig. 4. (a) Overview of **9d** full interaction maps, displaying all the preferential interactions for the adopted conformation and showing all probability contouring of 2, 4 and 6 times random. For colors: the H-bond donor in blue, acceptor in red and hydrophobic interaction are depicted in orange tridimensional scatterplots. (b) The emphasis for π-π stacking interaction of toluene groups from the molecule.

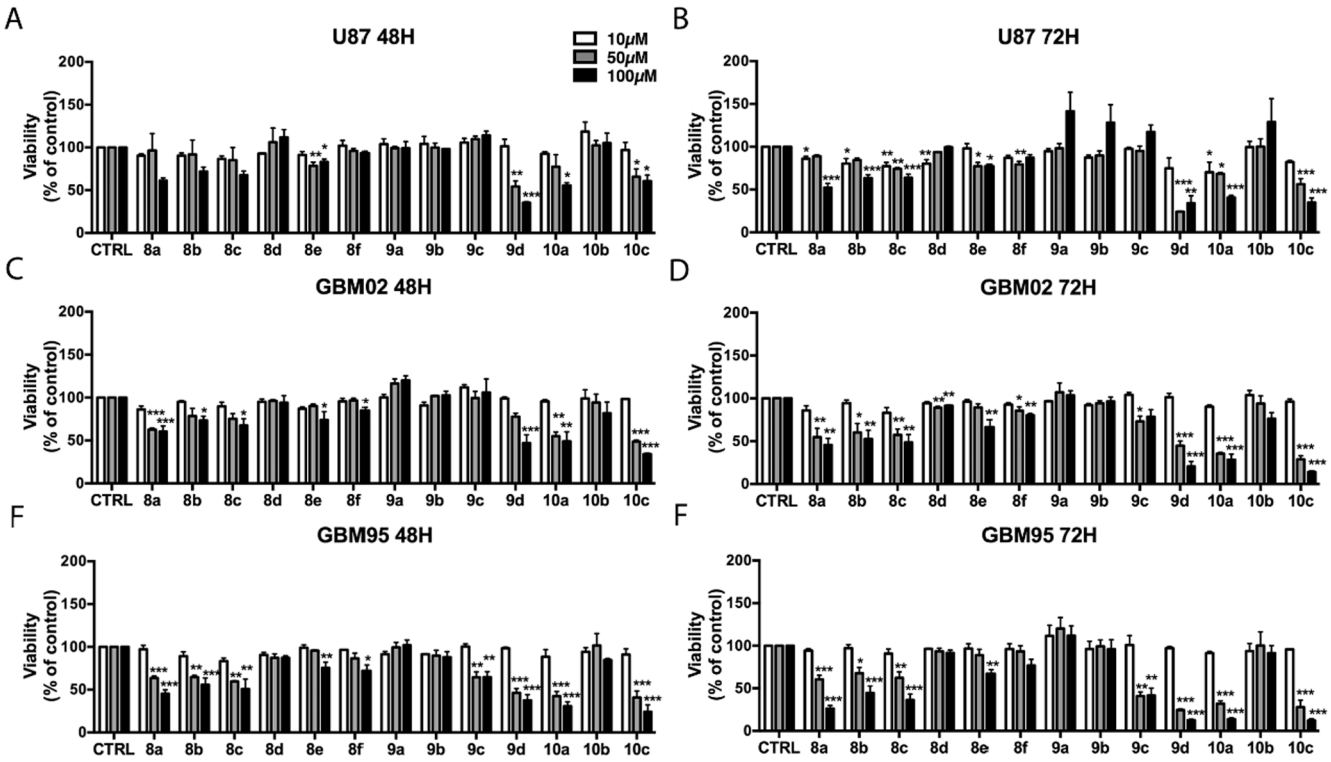

Fig. 5. Cytotoxicity of 1,2,3-triazole compounds in GBM cells. Graphs show the percentage of viable cells after treatment with 10, 50 and 100 μM of **8a-f, 9a-d** and **10a-c** compounds in U87 (A and B), GBM02 (C and D) and GBM95 (E and F) for 48 and 72 h determined by MTT assay. The values (A-F) represent mean and standard error of three independent experiments in triplicate. * $p < 0.05$; ** $p < 0.01$ *** $p < 0.001$.

Table 1
IC_{50} (μM) values of the compounds tested and **TMZ** for GBM and astrocyte (AST) cells treated for 48 and 72 h.

IC_{50}								
	GBM 95		GBM 02		U87		ASTH	
	48H	72H	48H	72H	48H	72H	48H	72H
8a	89.9	59.7	113.4	70	233.4	154.6	1179	2174
8b	107.5	95.3	238	95.8	298	183.5	685.2	1014
8c	83.9	70.8	179.9	76.3	218.8	146.5	2135	1745
8d	519.3	952.2	1416	743.5	–	2017	1285	5210
8e	398.6	247.3	301.5	243.5	329.7	268.8	–	–
8f	274.7	391.1	654.5	356.5	1414	394.5	–	–
9a	–	–	–	–	13,812	–	–	–
9b	589	2545	–	1578	8432	–	–	–
9c	142.5	57.6	–	263.1	–	–	–	–
9d	58	28.7	120.8	44.9	65.9	27.1	537	355.9
10a	44	30.3	81.7	38.2	140.5	72.4	8753	–
10b	754.8	1290	517.5	402.8	–	–	–	–
10c	40	29.5	57.3	30.6	130	57.2	–	144.1
TMZ	2643	1132	1712	624.8	–	–	993.3	949.8

linked to the methylenoxy moiety (**10a**) or to unsymmetrical tosyl-hydrazone triazole linked to such moiety (**9d**). The presence of the methylenoxy moiety is necessary since its removal, such as in **8f**, leads to drastic reduction of the activity of this compound in the cell lines tested. In the symmetrical bis-triazole **10a**, the presence of the aldehyde group was sufficient to maintain the activity, and its interconversion to other functional has disturbed the biological activity. It is possible that the bis-triazole group overcomes the need of tosyl-hydrazone, but it may also be related to physical chemical properties such as molecular weight or any other kind of interaction with the cell lines. On the other hand, in the case of the unsymmetrical compounds, the aldehyde group did not result in particular good activity, and its interconversion to other functional group was mandatory, especially with the tosyl-hydrazone. sulfonyl-hydrazones are privileged groups present in many compounds with anticancer activity [29]. Interestingly, other hydrazones derivatives, which also are considered privileged groups [30], did not improve the biological activity in the same way, reinforcing the role of the aryl-sulfone group. The other modifications performed at aldehyde-triazole **8a** did not enhance the pharmacological activity against the tested cell lines, the same observed in relation to B-ring

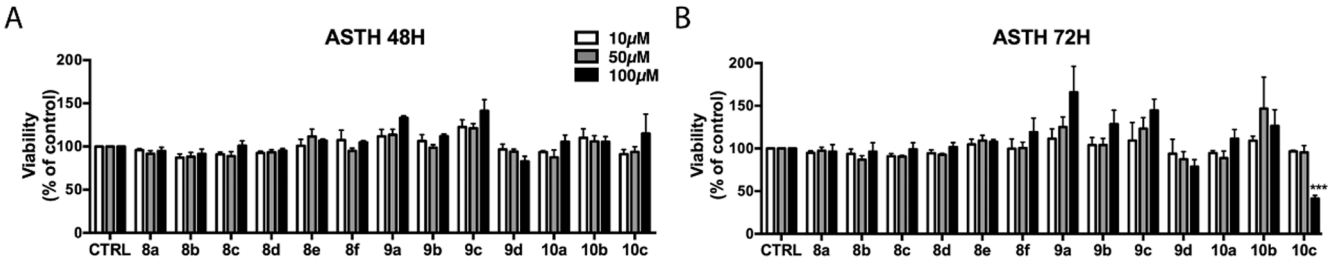

Fig. 6. Cytotoxicity of 1,2,3-triazole compounds against human astrocyte cells. Graphs show percentage of viable cells after the treatment for 48 (A) and 72 h (B) with **8a-f, 9a-d** and **10a-c** compounds in astrocyte cells determined by MTT assay. Values represent mean and standard error of three independent experiments in triplicate. * $p < 0.05$; ** $p < 0.01$ *** $p < 0.001$.

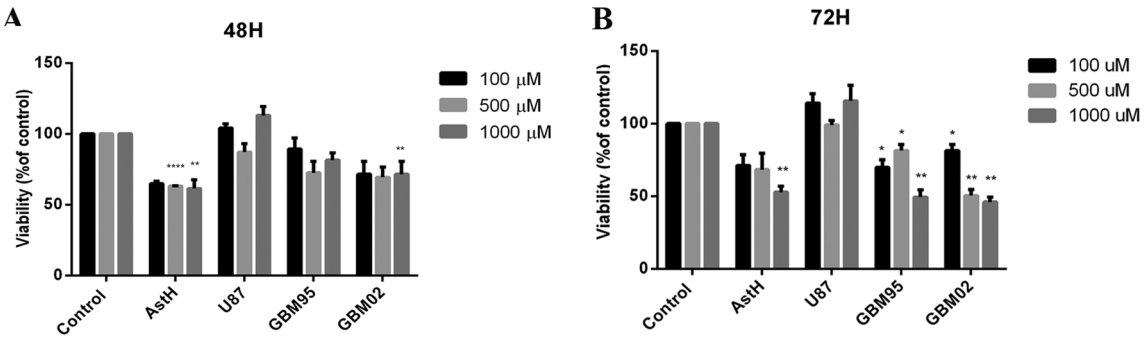

Fig. 7. Cytotoxicity of TMZ in GBM cells and human astrocytes. Graphs show the percentage of viable cells after treatment with 100, 500 and 1000 μM of TMZ in AstH,U87, GBM95 and GBM02 for 48 (A) and 72 h (B) determined by MTT assay. The values (A-B) represent mean and standard error of three independent experiments in triplicate.* $p < 0.05$; ** $p < 0.01$; **** $p < 0.0001$.

modifications of the compound **8a**. Since previous work have reported the anticancer activity of triazole derivatives containing propargyl phenol ethers groups [14,18], It seems to be an important spacer in the analyzed 1,4-disubstituted 1,2,3-triazole series.

2.2.2. *In silico analysis*

Successful drugs which target the central nervous system (CNS) normally have the following properties: molar weight ≤ 450; neutral or moderately positive charge at pH 7.4; logD 1–3; total number of hydrogen bonds ≤ 8; polar surface area ≤ 90 Å^2; and adequate absorption in the intestines [43–46]. Other desirable features for most drugs are metabolic stability [43], no hERG blockade-mediated cardiotoxicity [47], low hepatotoxicity [48], and no mutagenesis and carcinogenesis [49,50]. In order to assess the feasibility of the compounds studied herein for *in vivo* application, we performed an *in silico* analysis of physicochemical, pharmacokinetic, and toxicological properties using ADMET Predictor™ software. Although the software includes a direct predictor for blood-brain permeability, we also gave attention to other properties which greatly influence brain penetration, such as ionization state in the plasma, logD, hydrogen bonding capacity, and polar surface area. All compounds from this series were predicted to be hepatotoxic in humans. However, this cannot be considered a major problem in a drug discovery process, as many widely used drugs in the market are associated with case reports of idiosyncratic liver injury. Outstandingly, none of them were predicted to elicit lethal acute toxicity in rats. All the other results are presented in Table 2.

Compounds **8a**, **8b**, and **8c** were the most promising drug candidates, as they met all desirable criteria for CNS-acting drugs, despite high risk of liver toxicity and high rates of metabolic degradation. Additionally, compounds **10a** and **9d** met most of the criteria for CNS-acting drugs and were also considered to be good drug candidates along with **8a**, **8b**, and **8c**. Conversely, **10c** was predicted to be especially unsuitable to become a safe and active drug.

3. Conclusion

A series of 1,4-disubstituted-1,2,3-triazole derivatives was synthesized in good yields and were evaluated for different glioblastoma cell lines (GBM02, GBM95 and U87). Only compounds **8a**, **8b**, **8c**, **9d**, **10a**, and **10c** were able to reduce viability in the cell lines tested. The best results were obtained for compounds **9d** and **10a** with IC_{50} values of 27.1 μM for U87 cell line and 30.3 μM for the drug-resistant GBM95 human cell line, respectively. These compounds were also not toxic to astrocytes. All compounds had the structures confirmed by spectroscopic and spectrometric analyses and compound **9d** was additionally characterized by single crystal X-ray diffraction and the *E*-configuration of tosyl-hydrazone was confirmed. An *in silico* analysis of ADMET properties revealed that compounds **8a**, **8b**, **8c**, **9d**, and **10a** meet the criteria for central nervous system-acting drugs and therefore are potential new drug candidates.

4. Experimental part

4.1. *Materials and methods*

For the structural elucidation of the synthesized compounds, ^{1}H NMR and ^{13}C NMR spectra were recorded at ambient temperature on a Bruker Avance III spectrometer (operating at 400 MHz for ^{1}H NMR and 100 MHz for ^{13}C NMR). The chemical shifts (δ) were given in parts per million (ppm) from internal tetramethylsilane on the δ scale, multiplicity (s = singlet, d = doublet, t = triplet, q = quartet, m = multiplet). All coupling constants (J values) were given in Hz. Melting points were determined with an Electrothermal, analog model. Infrared spectra were performed using a Varian −3100 spectrometer. High resolution mass spectra were obtained by Bruker, MicrOTOF II instrument. Reactions were monitored by thin layer chromatography using Merck TLC Silica gel 60 F254. Silica gel column chromatography was performed over Merck Silica gel 60 Å (particle size: 0.040–0.063 mm, 230–400 mesh ASTM). All reagents used were commercially obtained and, where necessary, purified prior to use, such as THF and CH_2Cl_2 that were dried on a 4 Å molecular sieve.

4.2. *Synthesis of aryl-azides 13a-c*

4.2.1. *2-azidobenzaldehyde (**13a**)*

The 2-azidobenzaldehyde (**13a**) was prepared following the procedure of Feldman and co-workers [33]. A solution of 2–nitrobenzaldehyde (1.0 g, 6.6 mmol) and sodium azide (1.3 g, 20 mmol) in 15 mL of DMF was heated to 60 °C and stirred at that temperature for 96 h. The reaction mixture was diluted with diethyl ether (50 mL) and washed with water (4 × 25 mL). The combined organic layers were dried over Na_2SO_4, and concentrated in vacuum.

4.2.2. *2-azidobenzaldehyde (**13a**)*

The crude product was purified by flash column chromatography, using ethyl acetate/hexane (5:95) as eluent. The product was obtained as a pale yellow solid in 60% yield. MP: 36–37 °C. ^{1}H NMR (400 MHz, $CDCl_3$) δ 10.36 (s, 1H, CHO), 7.89 (dd, J = 7.8, 1.6 Hz, 1H, Ar-H), 7.65 – 7.60 (m, 1H, Ar-H), 7.30 – 7.21 (m, 2H, Ar-H). IR (KBr, ν_{max}): 2129 (N≡N), 1688 (C=O) cm^{-1}.

*4.2.2.1. Aryl-azides (**13b-c**).* The aryl-azides (**13b-c**) were prepared following the procedure of Wilkening and co-workers [34]. The aniline derivative (7.5 mmol) was dissolved in 5 mL of water and concentrated sulfuric acid (98%, 1.5 mL) and additional water (1.5 mL) was added. The suspension was cooled to 0 °C and a solution of $NaNO_2$ (7.6 mmol) of water (1.5 mL) was slowly added under constant stirring. After

Table 2
Prediction of physicochemical, pharmacokinetic, and toxicological properties of the compounds performed on ADMET Predictor™ software.

	MWt[a]	Charge[b]	logD[c]	HB[d]	PSA[e]	BP[f]	HJP[g]	Met[h]	Card[i]	Carc[j]	Mut[k]
8a	279	0 (100%)	2.88	4	57	Yes	H	H	No	0	No
8b	295	−1 (2%) 0 (98%)	2.47	6	77	Yes	H	I	No	0	No
8c	333	0 (100%)	2.84	5	66	Yes	H	H	No	0	No
8d	353	−1 (100%)	−0.71	8	104	Yes	H	L	No	0	No
8e	319	0 (100%)	3.45	5	70	Yes	H	I	No	0	Yes
8f	249	0 (100%)	2.91	3	48	Yes	H	H	No	0	No
9a	301	0 (100%)	4.09	3	40	Yes	H	H	No	0	No
9b	281	0 (100%)	2.49	5	60	Yes	H	H	No	0	Yes
9c	369	0 (100%)	4.33	6	64	Yes	H	H	Yes	M	Yes
9d	448	−1 (89%) 0 (11%)	2.93	8	98	Yes	H	L	Yes	0	No
10a	480	0 (100%)	2.83	8	114	Yes	H	I	No	0	No
10b	817	−2 (41%) −1 (50%) 0 (9%)	4.93	16	197	No	I	I	Yes	0	No
10c	695	0 (60%) +1 (40%)	−8.10	10	140	No	H	I	Yes	M	No

[a] Molar weight (g/mol).
[b] Charge at pH 7.4.
[c] Logarithm of octanol-water distribution coefficient taking into account all ionization states.
[d] Total number of hydrogen bond donors and acceptors.
[e] Polar surface area (Å^2).
[f] Brain penetration in rats (Yes or No).
[g] Human jejunal permeability (H, high; I, intermediate; L, low).
[h] Clearance rate catalyzed by CYPs (H, high; I, intermediate; L, low).
[i] Cardiotoxicity in humans, measured by the ability to inhibit hERG K^+ channel.
[j] Carcinogenicity in animal models (M, mouse; R, rat; 0, none).
[k] Mutagenicity, measured by the ability to induce mutations in at least 2 different *Salmonella typhimurium* strains in the Ames test.

15 min, NaN_3 (9.3 mmol) was added and the mixture was stirred for additional 0.5–1 h. The reaction mixture was extracted with ethyl acetate (3 × 20 mL) and the combined organic fractions were washed with water (50 mL). The organic layer was dried over Na_2SO_4 and concentrated under reduced pressure. The desired azides (**13b-c**) were obtained without further purification.

*4.2.2.2. 4-azidobenzoic acid (**13b**).* Yield 80%; light yellow solid. MP: 185 °C. ^{1}H NMR (400 MHz, DMSO-d_6) δ 12.97 (s, 1H, OH), 7.96 (d, J = 8.7 Hz, 2H, Ar-H), 7.22 (d, J = 8.7 Hz, 2H, Ar-H). IR (KBr, ν_{max}): 2105 (N≡N), *1284* (C—O) cm^{-1}.

*4.2.2.3. 6-azido-2H-chromen-2-one (**13c**).* Yield 94%; orange solid. MP: 159–161 °C. ^{1}H NMR (400 MHz, $CDCl_3$) δ 7.66 (d, J = 9.6 Hz, 1H, =CH), 7.34 (d, J = 8.8 Hz, 1H, Ar-H), 7.20 (dd, J = 8.8, 2.6 Hz, 1H, Ar-H), 7.12 (d, J = 2.6 Hz, 1H, Ar-H), 6.48 (d, J = 9.6 Hz, 1H, =CH). IR (KBr, ν_{max}): 2105 (N≡N), 1711(C=O) cm^{-1}.

4.3. Synthesis of alkynes 12a-d

Phenols (**11a-d**) (5.3 mmol) and anhydrous K_2CO_3 (10.6 mmol) were added in a 50 mL two-necked flask and dissolved in 15 mL acetonitrile. After 15 min, propargyl bromide (80% in toluene, 6.4 mmol) was slowly added and the reaction mixture was refluxed under N_2 atmosphere for 4.5 h. Then the mixture was diluted with water (25 mL) and extracted with dichloromethane (3 × 20 mL). The combined organic layers were dried over Na_2SO_4 and the solvent was concentrated under reduced pressure.

*4.3.1. (prop-2-yn-1-yloxy)benzene (**12a**).*
Yield 75%; yellow oil. ^{1}H NMR (400 MHz, $CDCl_3$) δ 7.33–7.29 (m, 2H, Ar-H), 6.99 (m, 3H, Ar-H), 4.70 (d, J = 2.4 Hz, 2H, CH_2), 2.52 (t, J = 2.4 Hz, 1H, CH). IR (KBr, ν_{max}): 3290 (≡CH), 2122 (C≡C) cm^{-1}.

*3-(prop-2-yn-1-yloxy)phenol (**12b**)*

The crude product was purified by flash column chromatography, using ethyl acetate/hexane (20:80). Yellow oil; yield 30%. ^{1}H NMR (400 MHz, $CDCl_3$) δ 7.15 (t, J = 8.0 Hz, 1H, Ar-H), 6.56 (dd, J = 8.1, 1.8 Hz, 1H, Ar-H), 6.50–6.46 (m, 2H, Ar-H), 4.88 (s, 1H, OH), 4.67 (d, J = 2.4 Hz, 2H, CH_2), 2.52 (t, J = 2.4 Hz, 1H, CH). IR (KBr, ν_{max}): 3287 (≡CH), 2122 (C≡C), 1281 (C—O) cm^{-1}.

*4.3.2. 1,3-bis(prop-2-yn-1-yloxy)benzene (**12c**)*
Two equivalents of anhydrous K_2CO_3 and propargylic bromide were required. The crude product was purified by flash column chromatography, using ethyl acetate/ hexane (20:80). White solid; yield 60%. MP: 38–39 °C. ^{1}H NMR (400 MHz, $CDCl_3$) δ 7.24–7.19 (m, 1H, Ar-H), 6.64–6.61 (m, 3H, Ar-H), 4.68 (d, J = 2.4 Hz, 4H, CH_2), 2.53 (t, J = 2.4 Hz, 2H, CH). IR (KBr, ν_{max}): 3288 (≡CH), 2122 (C≡C) cm^{-1}.

*4.3.3. 3-methoxy-4-(prop-2-yn-1-yloxy)benzaldehyde (**12d**).*
Yield 80%; white solid; MP: 86–87 °C. ^{1}H NMR (400 MHz, $CDCl_3$) δ 9.87 (s, 1H, CHO), 7.49–7.42 (m, 2H, Ar-H), 7.15 (d, J = 8.2 Hz, 1H, Ar-H), 4.87 (d, J = 2.4 Hz, 2H, CH_2), 3.94 (s, 3H, OCH_3), 2.56 (t, J = 2.4 Hz, 1H, CH). IR (KBr, ν_{max}): 3249 (≡CH), 2127 (C≡C), 1688 (C=O) cm^{-1}.

4.4. General procedure for the synthesis of triazoles (8a-f; 10a)

The triazoles were prepared following the procedure described by Sharpless et al. [32].

The alkyne (0.6 mmol) and aryl-azide (0.6 mmol) were added to a 1:1 mixture of water and tert-butyl alcohol (6 mL). Sodium ascorbate (0.06 mmol, in 200 μL of water) was added, followed by copper (II) sulfate pentahydrate (0.006 mmol, in 100 μL of water). The reaction mixture was stirred vigorously at room temperature and monitored by TLC until the reagents were completely consumed. At the end of the reaction the mixture was diluted with ice water (50 mL), the precipitate was collected by filtration, washed with cold water (2 × 25 mL) and dried under vacuum. If the precipitation doesn't work, the reaction the

mixture was extracted with 30 mL of dichloromethane and washed with water (2 × 25 mL). The combined organic layers were dried over $NaSO_4$ and evaporated under reduced pressure.

*4.4.1. 2-(4-(phenoxymethyl)-1H-1,2,3-triazol-1-yl)benzaldehyde (**8a**).*

Yield 65%; brown solid; Reaction time: 8 h; MP: 56–58 °C. ^{1}H NMR (400 MHz, $CDCl_3$) δ 9.92 (s, 1H, CHO), 8.13 (dd, J = 7.7, 1.5 Hz, 1H), 8.03 (s, 1H, triazole-H), 7.78 (td, J = 7.7, 1.6 Hz, 1H), 7.68 (t, J = 7.6 Hz, 1H), 7.54 (dd, J = 7.9, 1.0 Hz, 1H), 7.36–7.31 (m, 2H), 7.06–6.98 (m, 3H), 5.35 (s, 2H).^{13}C NMR (101 MHz, $CDCl_3$) δ 188.41, 158.12, 138.21, 134.69, 130.45, 130.13, 129.63, 125.48, 124.66, 121.54, 114.78, 61.89. IR (KBr, ν_{max}): 3093, 2867, 1703, 1600, 1496, 1239, 1042 cm^{-1}. HRMS(ESI) *m/z* calculated for $C_{16}H_{13}N_3O_2$ + Na $[M+Na]^+$, 302.0899; found 302.0900.

*4.4.2. 2-(4-((3-hydroxyphenoxy)methyl)-1H-1,2,3-triazol-1-yl) benzaldehyde (**8b**).*

Yield 60%; light brown solid; Reaction time: 8 h; MP: 112–114 °C. ^{1}H NMR (400 MHz, DMSO) δ 9.80 (s, 1H), 9.46 (s, 1H), 8.89 (s, 1H, triazole-H), 8.04 (dd, J = 7.9, 1.4 Hz, 1H), 7.92 (td, J = 7.8, 1.3 Hz, 1H), 7.78 (dd, J = 7.4, 5.8 Hz, 2H), 7.10 (t, J = 8.1 Hz, 1H), 6.53 (dd, J = 8.1, 2.0 Hz, 1H), 6.48 (t, J = 2.0 Hz, 1H), 6.41 (dd, J = 8.0, 1.8 Hz, 1H), 5.20 (s, 2H). ^{13}C NMR (101 MHz, DMSO) δ 189.83, 159.73, 159.06, 144.16, 137.94, 135.40, 130.56, 130.42, 130.35, 129.57, 127.04, 126.19, 108.82, 105.75, 102.55, 61.30. IR (KBr, ν_{max}): 3185, 3103, 2922, 1686, 1599, 1154, 1035 cm^{-1}. HRMS(ESI) *m/z* calculated for $C_{16}H_{13}N_3O_3$ + Na $[M+Na]^+$, 318.0849; found 318.0849.

*4.4.3. 2-(4-((3-(prop-2-yn-1-yloxy)phenoxy)methyl)-1H-1,2,3-triazol-1-yl)benzaldehyde (**8c**)*

The crude product was purified by flash column chromatography using ethyl acetate/hexane (20:80) as eluent. The product was obtained as a white solid in 40% yield. MP: 96–97 °C. ^{1}H NMR (400 MHz, $CDCl_3$) δ 9.92 (s, 1H), 8.13 (dd, J = 7.8, 1.5 Hz, 1H), 8.04 (s, 1H, triazole-H), 7.78 (td, J = 7.7, 1.6 Hz, 1H), 7.68 (t, J = 7.6 Hz, 1H), 7.54 (dd, J = 7.9, 0.9 Hz, 1H), 7.25–7.21 (m, 1H), 6.73–6.61 (m, 3H), 5.33 (s, 2H), 4.69 (d, J = 2.4 Hz, 2H), 2.53 (t, J = 2.4 Hz, 1H). ^{13}C NMR (101 MHz, $CDCl_3$) δ 188.39, 159.29, 158.86, 145.01, 138.18, 134.69, 130.44, 130.16, 129.64, 125.48, 124.78, 107.90, 107.81, 102.37, 78.44, 75.65, 61.97, 55.90, 29.71. IR (KBr, ν_{max}): 3262, 2920, 2117, 1693, 1589, 1143, 1040 cm^{-1}. HRMS(ESI) *m/z* calculated for $C_{19}H_{15}N_3O_3$ + Na $[M+Na]^+$, 356.1005; found 356.1006.

*4.4.4. 4-(4-((4-formyl-2-methoxyphenoxy)methyl)-1H-1,2,3-triazol-1-yl) benzoic acid (**8d**).*

Yield 80%; white solid; Reaction time: 8 h, MP: 238–239 °C. ^{1}H NMR (400 MHz, DMSO) δ 13.27 (s, 1H), 9.87 (s, 1H), 9.11 (s, 1H, triazole-H), 8.18–8.05 (m, 4H), 7.59 (dd, J = 8.2, 1.8 Hz, 1H), 7.46 – 7.41 (m, 2H), 5.38 (s, 2H), 3.82 (s, 3H). ^{13}C NMR (101 MHz, DMSO-d_6) δ 191.65, 152.88, 149.32, 143.67, 139.51, 129.93, 125.81, 123.43, 112.72, 109.72, 61.14, 55.14. IR (KBr, ν_{max}): 3144, 3086, 2827, 1632, 1588, 1504, 1422, 1262, 1140 cm^{-1}. HRMS(ESI) *m/z* calculated for $C_{18}H_{15}N_3O_5$ + Na $[M+Na]^+$, 376.0903; found 376.0904.

*4.4.5. 6-(4-(phenoxymethyl)-1H-1,2,3-triazol-1-yl)-2H-chromen-2-one (**8e**)*

The crude product was purified by flash column chromatography using ethyl acetate/hexane (40:60) as eluent. The product was obtained as an orange solid in 35% yield. Reaction time: 24 h; MP: 148–150 °C. ^{1}H NMR (400 MHz, $CDCl_3$) δ 8.09 (s, 1H, triazole-H), 7.86 (dd, J = 8.9, 2.5 Hz, 1H), 7.77 (d, J = 9.6 Hz, 1H), 7.49 (d, J = 8.9 Hz, 1H), 7.32 (dd, J = 8.7, 7.4 Hz, 1H), 7.05–6.97 (m, 2H), 6.55 (d, J = 9.6 Hz, 1H), 5.32 (s, 1H). ^{13}C NMR (101 MHz, $CDCl_3$) δ 160.13, 158.49, 154.07, 146.02, 142.83, 133.75, 130.09, 124.11, 121.94, 121.34, 120.03, 120.01, 118.94, 118.85, 115.16, 77.16, 62.31. IR (KBr, ν_{max}): 3055, 2920 1725, 1491, 1235, 1043 cm^{-1}. HRMS(ESI) *m/z* calculated for $C_{18}H_{13}N_3O_3$ + Na $[M+Na]^+$, 342.0849; found 342.0848.

*4.4.6. 2-(4-phenyl-1H-1,2,3-triazol-1-yl)benzaldehyde (**8f**)*

The crude product was purified by flash column chromatography using ethyl acetate/hexane (20:80) as eluent. The product was obtained as a white solid in 30% yield. Reaction time: 24 h; MP: 116–117 °C. ^{1}H NMR (400 MHz, $CDCl_3$) δ 10.00 (s, 1H), 8.18 (s, 1H, triazole-H), 8.14 (dd, J = 7.7, 1.1 Hz, 1H), 7.93 (d, J = 7.1 Hz, 2H), 7.80 (td, J = 7.7, 1.5 Hz, 1H), 7.69 (t, J = 7.6 Hz, 1H), 7.59 (d, J = 7.9 Hz, 1H), 7.48 (t, J = 7.5 Hz, 2H), 7.40 (t, J = 7.4 Hz, 1H). ^{13}C NMR (101 MHz, $CDCl_3$) δ 188.45, 148.56, 138.35, 134.69, 130.49, 130.10, 129.70, 129.54, 129.04, 128.77, 125.95, 125.36, 121.50. IR (KBr, ν_{max}): 3133, 2920 1685, 1597, 1455, 1018 cm^{-1}. HRMS(ESI) *m/z* calculated for $C_{15}H_{11}N_3O$ + Na $[M+Na]^+$, 272.0794; found 272.0794.

*4.4.7. 2,2′-(4,4′-((1,3-phenylenebis(oxy))bis(methylene))bis(1H-1,2,3-triazole-4,1 diyl)) dibenzaldehyde (**10a**)*

The crude product was purified by flash column chromatography using ethyl acetate/ hexane (20:80) as eluent. The product was obtained as a light yellow solid in 50% yield. Reaction time: 16 h, MP: 106–107 °C. ^{1}H NMR (400 MHz, $CDCl_3$) δ 9.91 (s, 2H), 8.11 (dd, J = 7.8, 1.5 Hz, 2H), 8.05 (s, 2H, triazole-H), 7.77 (td, J = 7.7, 1.6 Hz, 2H), 7.68 (t, J = 7.5 Hz, 2H), 7.54 (dd, J = 7.9, 0.9 Hz, 2H), 7.25 (t, J = 8.2 Hz, 1H), 6.73 (t, J = 2.3 Hz, 1H), 6.69 (dd, J = 8.2, 2.4 Hz, 1H), 5.33 (s, 4H). ^{13}C NMR (101 MHz, $CDCl_3$) δ 189.17, 160.18, 145.69, 138.87, 135.30, 131.14, 131.08, 130.83, 130.34, 126.18, 125.51, 108.51, 102.95, 62.87. IR (KBr, ν_{max}): 3117, 2918, 1688, 1598, 1154, 1036 cm^{-1}. HRMS(ESI) *m/z* calculated for $C_{26}H_{20}N_6O_4$ + Na $[M+Na]^+$, 503.1438; found 503.1438.

4.5. Synthesis of 1-(2-(difluoromethyl)phenyl)-4-(phenoxymethyl)-1H-1,2,3-triazole (9a)

The compound **9a** was prepared following the procedure described by Boechat [7].

To a solution of compound **8a** (0.06 g, 0.2 mmol) in anhydrous dichloromethane (2 mL), DAST (0.08 g, 0.52 mmol) was added dropwise under N_2 atmosphere. The reaction mixture was stirred for 24 h at room temperature. At the end of the reaction, it was added a saturated solution of $NaHCO_3$ (4 mL). The mixture was extracted with dichloromethane (2 × 10 mL), washed with brine (2 × 10 mL), dried (Na_2SO_4), and filtered. The solvent was evaporated under reduced pressure and the residue was purified by flash chromatography using ethyl acetate as eluent to give the product as an oil in 72% yield. ^{1}H NMR (400 MHz, $CDCl_3$) δ 7.93 (s, 1H, triazole-H), 7.87 (dd, J = 5.6, 3.7 Hz, 1H), 7.66 (dd, J = 5.8, 3.4 Hz, 2H), 7.48 (dd, J = 5.5, 3.6 Hz, 1H), 7.32 (dd, J = 8.7, 7.4 Hz, 2H), 7.05–6.98 (m, 3H,), 6.79 (t, J = 54.8 Hz, 1H, CHF_2), 5.32 (s, 2H). ^{13}C NMR (101 MHz, $CDCl_3$) δ 158.12, 144.94, 131.81, 130.33, 129.63, 127.14, 127.08, 127.01, 125.97, 124.78, 121.49, 114.83, 113.68, 111.30, 108.93, 61.89. R (KBr, ν_{max}): 1598, 1493, 1235, 1215, 1029 cm^{-1}. HRMS(ESI) *m/z* calculated for $C_{16}H_{13}F_2N_3O$ + Na $[M+Na]^+$, 324.0918; found 324.0919.

4.6. Synthesis of 2-(4-(phenoxymethyl)-1H-1,2,3-triazol-1-yl)phenyl) methanol (9b)

A mixture of compound **8a** (0.06 g, 0.21 mmol) in methanol (3 mL) was stirred until completely dissolved and then it was cooled in an ice bath. NaBH4 (0.02 g, 0.54 mmol) was added portionwise. After 30 min, the reaction mixture became clear, and TLC indicated the end of the reaction. The mixture was extracted with dichloromethane (15 mL), washed with water (2 × 10 mL). The organic phase was dried with Na_2SO_4, filtered and the solvent was evaporated under reduced pressure. The product (**9b**) was obtained as a white solid in 65% yield. MP: 94–96 °C. ^{1}H NMR (400 MHz, $CDCl_3$) δ 8.03 (s, 1H, triazole-H), 7.66 (d,

J = 7.1 Hz, 1H), 7.59–7.47 (m, 1H), 7.42 (d, J = 7.7 Hz, 1H), 7.35 (t, J = 7.9 Hz, 1H), 7.04 (dd, J = 15.7, 7.8 Hz, 1H), 5.35 (s, J = 11.2 Hz, 1H), 4.51 (d, J = 5.3 Hz, 1H), 3.39 (t, J = 5.8 Hz, 1H). ^{13}C NMR (101 MHz, $CDCl_3$) δ 158.13, 144.75, 135.92, 135.62, 131.61, 130.12, 129.65, 129.18, 124.45, 124.11, 121.49, 114.82, 61.93, 61.88. IR (KBr, ν_{max}): 3290, 2922, 1597, 1496, 1237, 1045 cm^{-1}. HRMS(ESI) *m/z* calculated for $C_{16}H_{15}N_3O_2$ + Na $[M+Na]^+$, 304.1056; found 304.1056.

4.7. General procedure for the synthesis of compounds (9c, 9d, 10b and 10c)

Compounds **8a** or **10a** (0.40 mmol, 1 eq) and hydrazine or imidazole (0.48 mmol, 1.2 eq) were added to a 10 mL round-bottomed flask and completely dissolved in methanol (3 mL). The reaction mixture was refluxed for 2 h at 60 °C. At the end of the reaction, the mixture was cooled in an ice bath. The precipitate was filtered and washed with cold water and ethanol.

4.7.1. (E)-4-(phenoxymethyl)-1-(2-((2-phenylhydrazono)methyl)phenyl)-1H-1,2,3-triazole (9c)

Yield 70%; white solid; MP: 128–129 °C. ^{1}H NMR (400 MHz, $CDCl_3$) δ 8.25 (dd, J = 8.0, 1.1 Hz, 1H), 7.89 (s, 1H), 7.77 (s, 1H), 7.56 (t, J = 7.1 Hz, 1H), 7.44 (td, J = 7.6, 1.4 Hz, 1H), 7.39–7.33 (m, 4H), 7.32–7.29 (m, 1H), 7.11–7.01 (m, 5H), 6.92 (t, J = 7.3 Hz, 1H), 5.37 (s, 2H). ^{13}C NMR (101 MHz, $CDCl_3$) δ 158.11, 144.05, 134.23, 131.29, 130.81, 130.14, 129.66, 129.32, 128.51, 126.57, 126.07, 121.45, 120.61, 114.92, 112.87, 61.85. IR (KBr, ν_{max}): 3226, 3036, 1738, 1598, 1493, 1237 cm^{-1}. HRMS(ESI) *m/z* calculated for $C_{22}H_{19}N_5O$ + Na $[M+Na]^+$, 392.1481; found 392.1482.

4.7.2. (E)-4-methyl-N′-(2-(4-(phenoxymethyl)-1H-1,2,3 triazol1yl) benzylidene)benzenesulfonohydrazide (9d)

Yield 65%; white solid; MP: 167–169 °C. ^{1}H NMR (400 MHz, CDCl3) δ 8.57 (s, 1H), 8.09 (dd, J = 7.3, 2.1 Hz, 1H), 7.82–7.79 (m, 3H), 7.54–7.48 (m, 3H), 7.35–7.27 (m, 4H), 7.05–6.95 (m, 3H), 5.26 (s, 2H), 2.39 (s, 3H). ^{13}C NMR (101 MHz, $CDCl_3$) δ 157.97, 144.63, 144.14, 141.29, 135.47, 130.66, 130.21, 129.65, 129.12, 127.84, 127.32, 125.74, 125.29, 121.51, 114.82, 61.58, 21.58. IR (KBr, ν_{max}): 3145, 1738, 1595, 1491, 1333, 1165 cm^{-1}. HRMS(ESI) *m/z* calculated for $C_{23}H_{21}N_5O_3S$ + Na $[M+Na]^+$, 470.1265; found 470.1261.

4.7.3. (N′,N″E,N′,N″E)-N′,N″-(((4,4′-((1,3-phenylenebis(oxy))bis (methylene))bis(1H-1,2,3-triazole-4,1-diyl))bis(2,1-phenylene))bis (methanylylidene))bis(4-methylbenzenesulfonohydrazide) product (10b)

Compound **10a** (0.1 g, 0.20 mmol) was treated with 2 equivalents p-toluenosufonyl-hydrazine (0.08 g, 0.45 mmol). Compound **10b** was obtained as white solid in 76% yield. MP: 135–137 °C. ^{1}H NMR (400 MHz, $CDCl_3$) δ 9.96 (s, 1H), 8.08 (dd, J = 7.5, 1.7 Hz, 1H), 7.84 (s, 1H), 7.77 (d, J = 8.3 Hz, 1H), 7.55–7.47 (m, 1H), 7.33 (dd, J = 7.6, 1.3 Hz, 1H), 7.22 (d, J = 8.1 Hz, 1H), 6.67 (dd, J = 8.2, 2.0 Hz, 1H), 6.55 (s, 1H), 5.28 (s, 1H), 3.51 (s, 1H), 2.37 (s, 1H). ^{13}C NMR (101 MHz, $CDCl_3$) δ 159.03, 144.26, 143.94, 141.13, 135.56, 135.28, 130.55, 130.30, 130.29, 129.58, 129.35, 127.76, 127.13, 125.81, 125.64, 109.44, 102.85, 62.06, 21.55. IR (KBr, ν_{max}): 3571, 3130, 1738, 1595, 1490, 1329, 1160 cm^{-1}. HRMS(ESI) *m/z* calculated for $C_{40}H_{36}N_{10}O_6S_2$ + Na $[M+Na]^+$, 839.2152; found 839.2153.

4.7.4. (N,N′E,N,N′E)-N,N′-(((4,4′-((1,3-phenylenebis(oxy))bis (methylene))bis(1H-1,2,3-triazole-4,1-diyl))bis(2,1-phenylene))bis (methanylylidene))bis(3-(1H-imidazol-1-yl)propan-1-amine) (10c)

The compound **10a** (0.1 g, 0.20 mmol) was treated with 2 equivalents 3-aminopropyl-imidazole (0.05 g, 0.42 mmol). Compound **10c** was obtained as a brown viscous oil in 60% yield. ^{1}H NMR (400 MHz, CDCl3) δ 8.16 (dd, J = 5.8, 3.6 Hz, 2H), 8.07 (s, 2H), 7.94 (s, 1H), 7.63–7.57 (m, 4H), 7.49 (s, 2H), 7.42 (dd, J = 5.8, 3.4 Hz, 2H), 7.03 (s, 2H), 6.94 (s, 2H), 6.73 (t, J = 2.3 Hz, 1H), 6.69 (d, J = 2.4 Hz, 1H), 6.67 (d, J = 2.4 Hz, 1H), 5.31 (s, 4H), 4.05 (t, J = 6.9 Hz, 4H), 3.48 (t, J = 5.8 Hz, 4H), 2.15–2.07 (m, 4H). ^{13}C NMR (101 MHz, $CDCl_3$) δ 159.54, 157.24, 144.58, 137.32, 136.45, 131.42, 131.24, 130.39, 130.30, 129.47, 128.70, 125.80, 125.12, 119.02, 107.83, 102.39, 77.16, 62.06, 57.84, 44.67, 31.94. IR (KBr, ν_{max}): 3111, 2930, 1641, 1592, 1490, 1455, 1379, 1148, 1033 cm^{-1}.

4.8. Biological evaluation

4.8.1. Glioblastoma and astrocyte cell culture

U87 cell line was obtained from the American Type Culture Collection (ATCC). GBM02 and GBM95 cell lines were established in the Laboratory of Cell Morphology (LMC) from the Federal University of Rio de Janeiro (UFRJ), as previously described [51] (Ethics Committee – CONEP 2340). Human astrocyte cells was prepared and cultured as previously described [52]. Those cells were cultivated in Dulbecco's modified eagle's medium (DMEM F12) supplemented with 10% of fetal bovine serum (SFB) and were maintained at 37 °C in 5% CO_2 and 95% air atmosphere.

4.8.2. MTT – Viability assay

Cellular viability was accessed by 3-(4,5-dimethylthiazol-2-yl)-2,5-diphenyl tetrazolium bromide (MTT) assay. Cells were cultured into 96-well plates at 1.5 × 10^4 cells/well concentration and then treated with 10, 50 and 100 μM of the compounds for 48 and 72 h. For the TMZ analysis cells were plated into 96-well plates at 1.5 × 10^4 cells/well concentration and then treated with 100,500 and 1000 μM of TMZ for 48 and 72 h. Dimethyl sulfoxide (DMSO) at the same dilution was used as control. In the end of the treatment MTT was added in each well in a final concentration of 5 mg/ml and incubated for 2 h at 37 °C. The formazan crystals produced were dissolved with DMSO and then the absorbance was measured at 570 nm using Victor 3 Perkin Elmer UV spectrophotometer. To calculate IC_{50} values a dose response-curve was plotted on a semi-log scale with concentrations (X-axis) versus percentage of cellular viability (Y-axis) and was fitted to a sigmoidal function. The curve fitting was performed using GraphPad Prism 6 [41].

4.9. In silico analysis

The 2D chemical structures of the compounds were drawn using ChemDraw (version Ultra 12.0) and were subjected to physicochemical, pharmacokinetic, and toxicological analyses on ADMET Predictor™ software (version 7.1; Simulations Plus, CA).

Acknowledgements

This study was financed in part by the Coordenação de Aperfeiçoamento de Pessoal de Nível Superior - Brasil (CAPES) - Finance Code 001

Appendix A. Supplementary material

Supplementary data to this article can be found online at https://doi.org/10.1016/j.bioorg.2018.10.003. These data include MOL files and InChiKeys of the most important compounds described in this article.

References

[1] F.R.S. Lima, S.A. Kahn, R.C. Soletti, D. Biasoli, T. Alves, A.C.C. da Fonseca, C. Garcia, L. Romão, J. Brito, R. Holanda-Afonso, J. Faria, H. Borges, V. Moura-Neto, Glioblastoma: therapeutic challenges, what lies ahead, Biochim. Biophys. Acta - Rev. Cancer 1826 (2) (2012) 338–349.

[2] M.B. Labib, J.N. Philoppes, P.F. Lamie, E.R. Ahmed, Azole-hydrazone derivatives: design, synthesis, in vitro biological evaluation, dual EGFR/HER2 inhibitory activity, cell cycle analysis and molecular docking study as anticancer agents, Bioorg.

Chem. 76 (2018) 67–80.
[3] S.S. Agarwala, J.M. Kirkwood, Temozolomide, a novel alkylating agent with activity in the central nervous system, may improve the treatment of advanced metastatic melanoma, Oncologist 5 (2) (2000) 144–151.
[4] R. Pinheiro, C. Braga, G. Santos, M.R. Bronze, M.J. Perry, R. Moreira, D. Brites, A.S. Falcão, Targeting gliomas: can a new alkylating hybrid compound make a difference? ACS Chem. Neurosci. 8 (1) (2016) 50–59.
[5] G.N. Castro, N. Cayado-Gutiérrez, F.C.M. Zoppino, M.A. Fanelli, F.D. Cuello-Carrión, M. Sottile, S.B. Nadin, D.R. Ciocca, Effects of temozolomide (TMZ) on the expression and interaction of heat shock proteins (HSPs) and DNA repair proteins in human malignant glioma cells, Cell Stress Chaperones 20 (2) (2015) 253–265.
[6] D. Dheer, V. Singh, R. Shankar, Medicinal attributes of 1,2,3-triazoles: current developments, Bioorg. Chem. 71 (2017) 30–54.
[7] N. Boechat, V.F. Ferreira, S.B. Ferreira, M.D.L.G. Ferreira, F.D.C. Da Silva, M.M. Bastos, M.D.S. Costa, M.C.S. Lourenço, A.C. Pinto, A.U. Krettli, A.C. Aguiar, B.M. Teixeira, N.V. Da Silva, P.R.C. Martins, F.A.F.M. Bezerra, A.L.S. Camilo, G.P. Da Silva, C.C.P. Costa, Novel 1,2,3-triazole derivatives for use against mycobacterium tuberculosis H37Rv (ATCC 27294) strain, J. Med. Chem. 54 (17) (2011) 5988–5999.
[8] M.F. Mady, G.E.A. Awad, K.B. Jørgensen, Ultrasound-assisted synthesis of novel 1,2,3-triazoles coupled diaryl sulfone moieties by the CuAAC reaction, and biological evaluation of them as antioxidant and antimicrobial agents, Eur. J. Med. Chem. 84 (2014) 433–443.
[9] B. Garudachari, A.M. Isloor, M.N. Satyanarayana, H.K. Fun, G. Hegde, Click chemistry approach: regioselective one-pot synthesis of some new 8-trifluoromethylquinoline based 1,2,3-triazoles as potent antimicrobial agents, Eur. J. Med. Chem. 74 (2014) 324–332.
[10] M.X. Song, X.Q. Deng, Recent developments on triazole nucleus in anticonvulsant compounds: a review, J. Enzyme Inhib. Med. Chem. 33 (1) (2018) 453–478.
[11] A.K. Jordão, V.F. Ferreira, T.M.L. Souza, G.G. De Souza Faria, V. MacHado, J.L. Abrantes, M.C.B.V. De Souza, A.C. Cunha, Synthesis and anti-HSV-1 activity of new 1,2,3-triazole derivatives, Bioorganic Med. Chem. 19 (6) (2011) 1860–1865.
[12] I. Mohammed, I.R. Kummetha, G. Singh, N. Sharova, G. Lichinchi, J. Dang, M. Stevenson, T.M. Rana, 1,2,3-triazoles as amide bioisosteres: discovery of a new class of potent HIV-1 Vif antagonists, J. Med. Chem. 59 (16) (2016) 7677–7682.
[13] R. Bollu, J.D. Palem, R. Bantu, V. Guguloth, L. Nagarapu, S. Polepalli, N. Jain, Rational design, synthesis and anti-proliferative evaluation of novel 1,4-benzoxazine-[1,2,3]triazole hybrids, Eur. J. Med. Chem. 89 (2014) 138–146.
[14] P. Yadav, K. Lal, A. Kumar, S.K. Guru, S. Jaglan, S. Bhushan, Green synthesis and anticancer potential of chalcone linked-1,2,3-triazoles, Eur. J. Med. Chem. 126 (2017) 944–953.
[15] E. Bonandi, M.S. Christodoulou, G. Fumagalli, D. Perdicchia, G. Rastelli, D. Passarella, The 1,2,3-triazole ring as a bioisostere in medicinal chemistry, Drug Discov. Today 22 (10) (2017) 1572–1581.
[16] S.G. Agalave, S.R. Maujan, V.S. Pore, Click chemistry: 1,2,3-triazoles as pharmacophores, Chem. Asian J. 6 (10) (2011) 2696–2718.
[17] M.S. Christodoulou, M. Mori, R. Pantano, R. Alfonsi, P. Infante, M. Botta, G. Damia, F. Ricci, P.A. Sotiropoulou, S. Liekens, B. Botta, D. Passarella, Click reaction as a tool to combine pharmacophores: the case of Vismodegib, Chempluschem 80 (6) (2015) 938–943.
[18] J. Doiron, A.H. Soultan, R. Richard, M.M. Touré, N. Picot, R. Richard, M. Čuperlović-Culf, G.A. Robichaud, M. Touaibia, Synthesis and structure-activity relationship of 1- and 2-substituted-1,2,3-triazole letrozole-based analogues as aromatase inhibitors, Eur. J. Med. Chem. 46 (9) (2011) 4010–4024.
[19] T. Srinivasa Reddy, H. Kulhari, V. Ganga Reddy, A.V. Subba Rao, V. Bansal, A. Kamal, R. Shukla, Synthesis and biological evaluation of pyrazolo–triazole hybrids as cytotoxic and apoptosis inducing agents, Org. Biomol. Chem. 13 (40) (2015) 10136–10149.
[20] J.A. Stefely, R. Palchaudhuri, P.A. Miller, R.J. Peterson, G.C. Moraski, P.J. Hergenrother, M.J. Miller, N -((1-benzyl-1 H -1,2,3-triazol-4-yl)methyl)arylamide as a new scaffold that provides rapid access to antimicrotubule agents: Synthesis and evaluation of antiproliferative activity against select cancer cell lines, J. Med. Chem. 53 (8) (2010) 3389–3395.
[21] A. Padmaja, D. Pedamalakondaiah, G. Sravya, G.M. Reddy, M.V.J. Kumar, Synthesis and antioxidant activity of a new class of sulfone/sulfonamide-linked bis(oxadiazoles), bis(thiadiazoles), and bis(triazoles), Med. Chem. Res. 24 (5) (2015) 2011–2020.
[22] H. Elamari, R. Slimi, G.G. Chabot, L. Quentin, D. Scherman, C. Girard, Synthesis and in vitro evaluation of potential anticancer activity of mono- and bis-1,2,3-triazole derivatives of bis-alkynes, Eur. J. Med. Chem. 60 (2013) 360–364.
[23] K.M. Dawood, B.F. Abdel-Wahab, M.A. Raslan, Synthesis and applications of bi- and bis-triazole systems, Arkivoc 2018 (1) (2018) 179–215.
[24] B. Sever, M.D. Altintop, G. Kuş, M. Özkurt, A. Özdemir, Z.A. Kaplancikli, Indomethacin based new triazolothiadiazine derivatives: synthesis, evaluation of their anticancer effects on T98 human glioma cell line related to COX-2 inhibition and docking studies, Eur. J. Med. Chem. 113 (2016) 179–186.
[25] A. Ogino, E. Sano, Y. Ochiai, S. Yamamuro, S. Tashiro, K. Yachi, T. Ohta, T. Fukushima, Y. Okamoto, K. Tsumoto, T. Ueda, A. Yoshino, Y. Katayama, Efficacy of ribavirin against malignant glioma cell lines, Oncol. Lett. 8 (6) (2014) 2469–2474.
[26] S.J. Enoch, C.M. Ellison, T.W. Schultz, M.T.D. Cronin, A review of the electrophilic reaction chemistry involved in covalent protein binding relevant to toxicity, Crit. Rev. Toxicol. 41 (9) (2010) 783–802.
[27] D.W. Domaille, J.N. Cha, Aniline-terminated DNA catalyzes rapid DNA-hydrazone formation at physiological pH, Chem. Commun. 50 (29) (2014) 3831–3833.
[28] R. Narang, B. Narasimhan, S. Sharma, A review on biological activities and chemical synthesis of hydrazide derivatives, Curr. Med. Chem. 19 (4) (2012) 569–612.
[29] A. Queen, P. Khan, D. Idrees, A. Azam, M.I. Hassan, Biological evaluation of p-toluene sulphonylhydrazone as carbonic anhydrase IX inhibitors: an approach to fight hypoxia-induced tumors, Int. J. Biol. Macromol. 106 (2018) 840–850.
[30] S. Rollas, Ş.G. Küçükgüzel, Biological activities of hydrazone derivatives, Molecules 12 (8) (2007) 1910–1939.
[31] C.D. Sessler, M. Rahm, S. Becker, J.M. Goldberg, F. Wang, S.J. Lippard, CF2H, a hydrogen bond donor, J. Am. Chem. Soc. 139 (27) (2017) 9325–9332.
[32] V.V. Rostovtsev, L.G. Green, V.V. Fokin, K.B. Sharpless, A stepwise huisgen cycloaddition process catalyzed by copper (I): regioselective ligation of azides and terminal alkynes, Angew. Chem. Int. Ed. 41 (14) (2002) 2596–2599.
[33] K.S. Feldman, I.Y. Gonzalez, C.M. Glinkerman, Intramolecular [3 + 2] cyclocondensations of alkenes with indolidenes and indolidenium cations, J. Am. Chem. Soc. 136 (43) (2014) 15138–15141.
[34] I. Wilkening, G. del Signore, C.P.R. Hackenberger, Synthesis of phosphonamidate peptides by Staudinger reactions of silylated phosphinic acids and esters, Chem. Commun. 47 (1) (2011) 349–351.
[35] C. Su, Z. Ding, X. Liu, K. Cui, J. Ma, Cu (I) -promoted one-pot ' Click-S N Ar reaction ' of nitrobenzaldehydes, vol. 7911, no. May, 2016.
[36] S. Tsuzuki, K. Honda, T. Uchimaru, M. Mikami, Ab initio calculations of structures and interaction energies of toluene dimers including CCSD(T) level electron correlation correction, J. Chem. Phys. (2005).
[37] G.V. Janjić, D.B. Ninković, S.D. Zarić, Influence of supramolecular structures in crystals on parallel stacking interactions between pyridine molecules, Acta Crystallogr. Sect. B Struct. Sci. Cryst. Eng. Mater. 69 (4) (2013) 389–394.
[38] C.R. Martinez, B.L. Iverson, Rethinking the term 'pi-stacking', Chem. Sci. 3 (7) (2012) 2191.
[39] C.H. Ryu, W.S. Yoon, K.Y. Park, S.M. Kim, J.Y. Lim, J.S. Woo, C.H. Jeong, Y. Hou, S.S. Jeun, Valproic acid downregulates the expression of MGMT and sensitizes temozolomide-resistant glioma cells, J. Biomed. Biotechnol. 2012 (2012).
[40] J. Balça-Silva, D. Matias, A. Do Carmo, H. Girão, V. Moura-Neto, A.B. Sarmento-Ribeiro, M.C. Lopes, Tamoxifen in combination with temozolomide induce a synergistic inhibition of PKC-pan in GBM cell lines, Biochim. Biophys. Acta - Gen. Subj. 1850 (4) (2015) 722–732.
[41] D. Matias, J. Balça-Silva, L.G. Dubois, B. Pontes, V.P. Ferrer, L. Rosário, A. do Carmo, J. Echevarria-Lima, A.B. Sarmento-Ribeiro, M.C. Lopes, V. Moura-Neto, Dual treatment with shikonin and temozolomide reduces glioblastoma tumor growth, migration and glial-to-mesenchymal transition, Cell. Oncol. 40 (3) (2017) 247–261.
[42] S.A. Kahn, D. Biasoli, C. Garcia, L.H.M. Geraldo, B. Pontes, M. Sobrinho, A. Carina, B. Frauches, L. Romão, R.C. Soletti, S. Assunção, F. Tovar-moll, J.M. De Souza, F.R.S. Lima, G. Anderluh, V. Moura-neto, Equinatoxin II potentiates glioblastoma cell death and, Curr. Top. Med. Chem. (2012) 2082–2093.
[43] H. Pajouhesh, G.R. Lenz, Medicinal chemical properties of successful central nervous system drugs, NeuroRX 2 (4) (Oct. 2005) 541–553.
[44] W.M. Pardridge, Transport of small molecules through the blood-brain barrier: biology and methodology, Adv. Drug Deliv. Rev. 15 (1–3) (1995) 5–36.
[45] S.A. Pathan, Z. Iqbal, S.M.A. Zaidi, S. Talegaonkar, D. Vohra, G.K. Jain, A. Azeem, N. Jain, J.R. Lalani, R.K. Khar, F.J. Ahmad, CNS drug delivery systems: novel approaches, Recent Pat. Drug Deliv. Formul. 3 (1) (2009) 71–89.
[46] H. Van De Waterbeemd, G. Camenisch, G. Folkers, J.R. Chretien, O.A. Raevsky, Estimation of blood-brain barrier crossing of drugs using molecular size and shape, and H-bonding descriptors estimation of blood-brain barrier crossing of drugs using molecular size and shape, and H-bonding descriptors, J. Drug Targering 6 (2) (1998) 151–165.
[47] P.J. Stansfeld, P. Gedeck, M. Gosling, B. Cox, J.S. Mitcheson, M.J. Sutcliffe, Drug block of the hERG potassium channel: Insight from modeling, Proteins Struct. Funct. Bioinforma. 68 (2) (2007) 568–580.
[48] W.M. Lee, Drug-induced hepatotoxicity, N. Engl. J. Med. 349 (5) (2003) 474–485.
[49] C.C. Harris, The carcinogenicity of anticancer drugs: a hazard in man, Cancer 37 (2 Suppl) (1976) 1014–1023.
[50] K. Mortelmans, E. Zeiger, The Ames Salmonella/microsome mutagenicity assay, Mutat. Res. 455 (2000) 29–60.
[51] J. Faria, L. Romão, S. Martins, T. Alves, F.A. Mendes, G.P. De Faria, R. Hollanda, C. Takiya, L. Chimelli, V. Morandi, J.M. De Souza, J.G. Abreu, V.M. Neto, Interactive properties of human glioblastoma cells with brain neurons in culture and neuronal modulation of glial laminin organization, Differentiation 74 (9–10) (2006) 562–572.
[52] C. Garcia, G.G. Dubois, L.L. Xavier, H.H. Geraldo, C.C.C. da Fonseca, H.H. Correia, F. Meirelles, G. Ventura, L. Romão, S.H.S. Canedo, M.M. de Souza, L.R.L. de Menezes, V. Moura-Neto, F. Tovar-Moll, S.R.S. Lima, The orthotopic xenotransplant of human glioblastoma successfully recapitulates glioblastoma-microenvironment interactions in a non-immunosuppressed mouse model, BMC Cancer 14 (1) (2014) 1–11.